ELECTRIC EFFECTS ON CONDUCTING NEWTONIAN AND VISCOELASTIC DROPLETS

Nicolao Cerqueira Lima
Marcos Akira d'Ávila
University of Campinas – Unicamp – School of Mechanical Engineering
Mendeleyev St. 200, Cidade Universitária "Zeferino Vaz", Barão Geraldo District, Campinas – SP 13083-970
nicolaol@hotmail.com
madavila@fem.unicamp.br

Abstract. *In the present work, a solver on the open CFD software OpenFOAM was implemented, based on the leaky dielectric model, in order to study the effects of an electric field in conducting droplets. These simulations were performed considering both Newtonian and viscoelastic fluids. The Giesekus constitutive equation was used to describe the viscoelastic behavior. The results of the deformation of a conducting droplet were compared to analytical results, for Newtonian fluids, and with theoretical results, for viscoelastic ones. It was observed that the most important parameter that influences the deformation of the drop, indeed, is the electric field. Other parameters, such as the conductivity, permittivity and elasticity, also play a role on the deformation magnitude. Due to the applied electric field, it was observed that the droplet deforms on a stable spheroidal form.. For viscoelastic fluids the deformation was reduced with the increase of the relaxation time. Also, it was observed the formation of four vortexes inside and outside the droplet, which agrees with experimental observations.*

Keywords: Electrohydrodynamic, simulation, viscoelastic fluids, CFD, OpenFOAM.

1. INTRODUCTION

Over the past decades, the effects of an electric field over fluids have been studied from a theoretical point of view in order to develop new processes. The understanding of the so called electrohydrodynamic effects has begun with the works of Taylor (1964) that observed the motion of a conducting drop when it is inserted in a uniform electric field. After these studies, many processes aiming the study of electrohydrodynamics were developed. Among them are the electrohydrodynamic atomization, electrospinning, liquid dispersion, ink jet printing, and others (Saville, 1997).

However, there is some difficulty in improving such processes due to the high number of parameters involved and to the complexity of the flow (Thompson, *et al.*, 2007). Therefore, theoretical studies about the influence of the parameters are necessary. So, the simulation of such processes became an advantageous option, once it facilitates the change of parameters and, thereby, avoids material expenses in the testing phase.

The complexity involved in these processes encouraged the development of models that describe the electric effects on fluids. So, theoretical studies as well as physical models have come to be developed and, subsequently, the leaky dielectric model was stated by Taylor, completed by Melcher and reviewed by Saville (Saville, 1997).

The electrohydrodynamic model deals basically with the coupling of the mass and momentum equations with Maxwell equations. In the presence of an electric field the molecules of the fluid polarize and, when dealing with a homogeneous dielectric medium, the charge accumulates only at the surface. For a conducting fluid, however, charged ions or free charges migrate instantly to the surface, resulting in an electric charge density, so that there is no charge within the fluid (Herrera, *et al.*, 2011). The consequence is the appearance of an electric surface force that will deform the fluid, until surface, viscous and elastic tensions provide the necessary balance. In leaky dielectric fluids, the surface charge density modifies the electric field producing tangential components for the electric forces, differently from those produced by purely dielectrics or perfect conductors, which are perpendicular to the surface.

Many authors have implemented the leaky dielectric model and simulated electrohydrodynamic problems (Feng, 2002; Tomar, *et al.*, 2007; Herrera, *et al.*, 2011). Sherwood (1988) performed experimental and numerical simulations of the deformation and breakup of a droplet rounded by a fluid with the same density. He observed that the deformation remained stable even with high values of electric fields. Feng and Scott (1996) made simulation studies using the leaky dielectric model of droplet deformation for a range of electric field intensities. Their results were consistent with experimental observations. The difficulty arrives, however, when dealing with the droplet interface (since it is a two-phase problem). The front tracking method was used, for the interface treatment, by Hua *et al.* (2008) in order to analyze three different models: the leaky dielectric, purely dielectric and perfect conductor. The results were close to analytical ones. Herrera, *et al.* (2011) used the VOF (volume of fluid) method to make three-dimensional simulations of a conducting drop. They observed similar results compared to the analytical model proposed by Taylor (1966).

Little has been done about electrohydrodynamic flow simulations of viscoelastic fluids. The difficulty arrives in modeling the problem due to the complexity of the equations involved. Favero (2009) and Favero, *et al.* (2010a) implemented a solver in the free package OpenFOAM, which is capable of simulating viscoelastic fluid flows. The

solver allows different constitutive equations and it was validated using the classical problem of a planar contraction. Favero, *et al.* (2010b) expended the solver for multiphase flows using the VOF method. In that case, the die swell experiment was simulated and the results were consistent with experimental observations.

The implementation of an electrohydrodynamic solver together with the viscoelastic multiphase one is a great progress in the field of fluid flow simulation, and will allow more studies about processes such as electrospinning, as well as more general studies concerning the effect of the parameters on viscoelastic electrohydrodynamic flows.

2. METHODOLOGY

In this section, the mathematical formulation for electrhydrodynamic flows, as well as the Giesekus constitutive equation, used for simulating viscoelastic flows, is presented. A general description of the problem of a conducting droplet and the boundary conditions is also presented.

2.1 Mathematical model

The general governing equations in a viscoelastic problem, considering isothermal and incompressible fluids are the mass conservation (continuity equation) given by Eq. (1):

$$\nabla \cdot \boldsymbol{U} = 0 \tag{1}$$

where $\boldsymbol{U}$ is the velocity vector, and the momentum conservation equation in its conservative form is given by Eq. (2):

$$\frac{\partial(\rho \boldsymbol{U})}{\partial t} + \nabla \cdot (\rho \boldsymbol{U}\boldsymbol{U}) = -\nabla p + \nabla \cdot (\boldsymbol{\tau^m} + \boldsymbol{\tau^e}) + \rho \mathbf{g} \tag{2}$$

where ρ is the fluid density, p is the pressure, $\boldsymbol{\tau}^m$ is the stress tensor, $\boldsymbol{\tau}^e$ is the electric stress tensor and $\mathbf{g}$ is the gravitational acceleration vector. The stress tensor is given by two different contributions, one for the solvent $\boldsymbol{\tau}_S$ and one for the polymer $\boldsymbol{\tau}_P$. So, the stress tensor can be written as $\boldsymbol{\tau}^m = \boldsymbol{\tau}_S + \boldsymbol{\tau}_P$ (Favero, *et al.*, 2010a), where:

$$\boldsymbol{\tau}_S = 2\eta_S \boldsymbol{S} \tag{3}$$

and $\boldsymbol{\tau}_P$ is the solution of a specified constitutive equation. In the present work, the Giesekus equation was used, and it's given by Eq. (4) (Bird, *et al.*, 1987):

$$\boldsymbol{\tau}_{P_K} + \lambda_K \, \check{\boldsymbol{\tau}}_{P_K} + \alpha_K \frac{\lambda_K}{\eta_{P_K}} \left(\boldsymbol{\tau}_{P_K} \cdot \boldsymbol{\tau}_{P_K} \right) = 2\eta_{P_K} \boldsymbol{S} \tag{4}$$

In the above equations η_S is the solvent viscosity, λ is the relaxation time, $\check{\boldsymbol{\tau}}_P$ is the upper convected derivative applied to the stress tensor, α is the mobility factor of the relaxation mode K (Giesekus, 1982), η_P is the polymer viscosity at zero share rate, and $\boldsymbol{S}$ is the deformation rate tensor given by:

$$\boldsymbol{S} = \frac{1}{2} (\nabla \boldsymbol{U} + [\nabla \boldsymbol{U}]^T) \tag{5}$$

The relaxation mode K varies from $1 \leq K \leq N$, where N is the number of relaxation modes. In this work it has been set $N = 1$. If more relaxation modes were considered the final value of $\boldsymbol{\tau}_P$ would be given as the sum of the contributions of the individual relaxation modes (Favero, 2009). The upper convected derivative in Eq. (4) is given by:

$$\check{\boldsymbol{\tau}}_{P_K} = \frac{D\boldsymbol{\tau}_{P_K}}{Dt} - \left[\nabla \boldsymbol{U}^T \cdot \boldsymbol{\tau}_{P_K} \right] - \left[\boldsymbol{\tau}_{P_K} \cdot \nabla \boldsymbol{U} \right] \tag{6}$$

where $D\boldsymbol{\tau}_{P_K}/Dt$ is the substantive derivative given by:

$$\frac{D\boldsymbol{\tau}_{P_K}}{Dt} = \frac{\partial \boldsymbol{\tau}_{P_K}}{\partial t} + \boldsymbol{U} \cdot \nabla \boldsymbol{\tau}_{P_K} \tag{7}$$

In order to describe the electrohydrodynamic behavior of the flow, the Maxwell's equations are used. In these kinds of flows the magnetic effects can be neglected, since it is assumed, in the leaky dielectric model, that the charges migrate instantaneously to the surface. Thus, the electric field is irrotational and it can be described as a potential gradient, as shown in Eq. (8) (Griffiths, 1999):

$$E = -\nabla\phi \tag{8}$$

where E is the electric field and ϕ is the electric potential. The Poisson equation is given by (Herrera, *et al.*, 2011):

$$\nabla \cdot (\epsilon E) = \rho_e \tag{9}$$

where ϵ is the permittivity of the fluid and ρ_e is the volumetric charge density.

In Eq. (2) the τ^e refers to the Maxwell stress tensor. One way of evaluating its relationship with the electric force is to assume that the force on the free charges as well as the force on the dipoles, formed due to the molecules polarization, is transferred directly to the fluid. So, the electric force per unit volume can be written as the divergence of the Maxwell stress tensor, which is given by (Saville, 1997):

$$\tau^e = \epsilon \left(EE - \frac{1}{2} E^2 \mathbb{I} \right) \tag{10}$$

where $\mathbb{I}$ is the identity tensor. And, thus, the electric force F_e can be written as:

$$F_e = \rho_e E - \frac{1}{2} E^2 \nabla\epsilon \tag{11}$$

Finally, an equation is necessary to describe the charge conservation (Herrera, *et al.*, 2011; Poppel, 2010).

$$\frac{\partial \rho_e}{\partial t} + \nabla \cdot (\sigma E + \rho_e U) = 0 \tag{12}$$

The first term inside the divergence is related to the charge conduction, while the second term is related to the charge convection. The Greek letter σ represents the conductivity of the fluid.

Since we´re dealing with a two-phase problem, a method that can treat with the free surface interface is required. The OpenFOAM package uses the VOF methodology developed by Hirt and Nichols (1981). It consists on an indicator function α_1 that allows us to know whether the control volume is totally filled with one fluid by making $\alpha_1 = 1$ or another fluid by making $\alpha_1 = 0$. The interface is described by values of α_1 ranging from $0 < \alpha_1 < 1$. Thus, we can describe the properties ρ, ϵ, μ and σ of both fluids by the following relationship:

$$\theta = \alpha_1 \theta_{phase\,1} + (1 - \alpha_1)\theta_{phase\,2} \tag{13}$$

where θ is a generic property. The indicator function must satisfy a transport equation given by (Hirt, Nichols, 1981):

$$\frac{\partial \alpha_1}{\partial t} + \nabla \cdot (\alpha_1 U) + \nabla \cdot (\alpha_1(1 - \alpha_1)U_r) = 0 \tag{14}$$

Here, U_r is the relative velocity vector between phase 1 and 2 and it's given by $U_r = U_1 - U_2$. The last term in Eq. (14) is only activated on the interface since $\alpha_1(1 - \alpha_1) = 0$ for $\alpha_1 = 1$ and $\alpha_1 = 0$.

One last term must be included in Eq. (2). This one is related to the surface tension, and it's given by:

$$\gamma\kappa\nabla\alpha_1 \tag{15}$$

where γ is the surface tension and κ represents the curvature of the free surface imposed by the equation (Hirt, Nichols, 1981):

$$\kappa = -\nabla \cdot \left(\frac{\nabla\alpha_1}{|\nabla\alpha_1|} \right) \tag{16}$$

2.2 Problem description

The problem consists in evaluating the deformation rate of a droplet inserted between two parallel plates, where an electric potential is being applied. Since a potential difference exists, an electric field will be generated between the plates, which will eventually ionize and/or polarize the droplet. An electric force will appear at the droplet surface deforming it. Figure 1 shows a sketch of the problem:
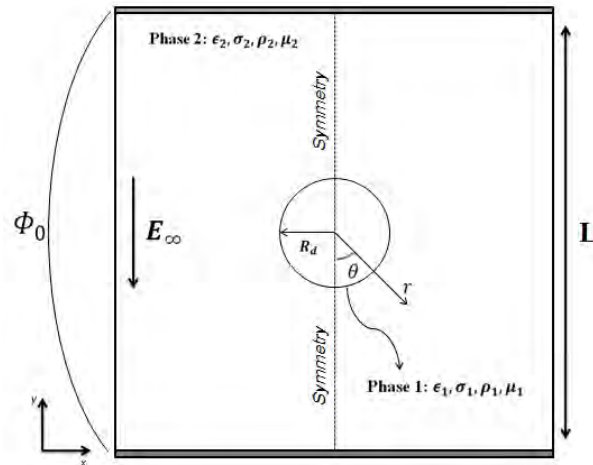
Figure 1. Sketch of the conducting droplet inserted in an electric field problem.

The problem was considered symmetric, with the symmetry axis perpendicular to the plates and passing at the center of the drop. On the upper plate a higher potential was applied, generating an external electric field E_∞ from top to bottom. Near the drop, the electric field intensity will change due to the accumulated charge density on the surface.

Experimentally, it was observed that a uniform electric field deforms a conducting droplet immersed in a non-conducting fluid in a prolate spheroid (Taylor, 1964). When both fluids are purely dielectric there will also be a deformation, and that will be always in a prolate shape. However, in some cases, due to the fluids conductivity, it may be observed an oblate deformation (Taylor, 1966). The two kinds of deformation can be seen in Fig. 2:
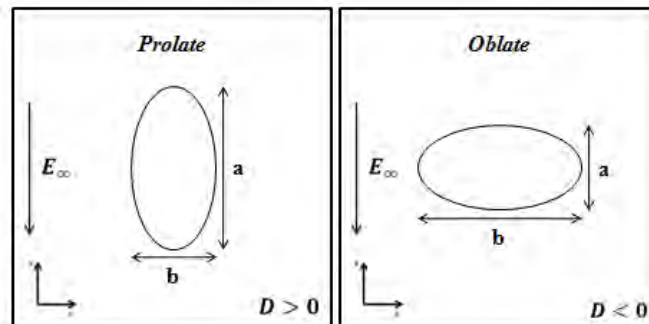

Figure 2. Deformation types for a droplet inserted in an electric field.

Taylor (1966) characterized the total deformation of the drop by means of a D parameter defined as follows:

$$D = \frac{a - b}{a + b} \tag{17}$$

where a and b represent the deformation size parallel and perpendicular to the external electric field, respectively. Thus, for $D > 0$ the drop deformed into a prolate shape, and for $D < 0$ it deformed into an oblate shape.

Taylor (1966) also expressed another equation for the droplet deformation valid only for small deformations (Ha, Yang, 1995; Feng, Scott, 1996). The last one is a function of both fluid properties, and is given by:

$$D = \frac{9}{16} \frac{Ca_E}{(2 + R)^2} \left[1 + R^2 - 2Q + \frac{3}{5}(R - Q)\frac{2 + 3\beta}{1 + \beta} \right] \tag{18}$$

where $R = \sigma_1/\sigma_2$, $Q = \epsilon_1/\epsilon_2$ and $\beta = \mu_1/\mu_2$ stands for the ratio of the inner fluid to the outer conductivities, permittivities and viscosities, respectively. $Ca_E = E_\infty^2 R_d \epsilon_2/\gamma$ is the capillary number, where $E_\infty = \Delta\phi/L$, being L the distance between the plates, and R_d is the initial droplet radius.

The capillary number represents the ratio between the electric forces and interfacial tensions. In this work, the same viscosities for both fluids were applied, so $\beta = 1$.

2.3 Boundary Conditions

For the distance between the plates it was assigned a value of $L = 0.1$ m, because it corresponds to the same dimension used in the literature (Hua, *et al.*, 2008). Since the interest is to evaluate the electrical parameters effect, the ratio between the densities for the inner fluid to the outer was set to 1 ($\rho_1/\rho_2 = 1$). The boundary conditions were applied accordingly to the boundary types available on the OpenFOAM free source package. Figure 3 shows the locations where the boundary conditions were applied:
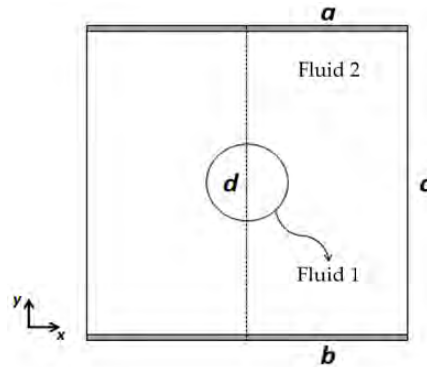

Figure 3. Boundaries of the droplet problem.

The conditions for pressure, velocity, volume fraction, electric charge density and electric potential imposed for the a and b boundaries are shown in Tab. 1, where a no-slip condition was applied (wall condition):

Table 1. Conditions imposed for the a and b boundaries.

B. C.	p	U	α_1	ρ_e	ϕ
a	$\nabla p = 0$	$U = (0,0,0)$	$\nabla \alpha_1 = 0$	$\nabla \rho_e = 0$	$\phi = \phi_0$
b	$\nabla p = 0$	$U = (0,0,0)$	$\nabla \alpha_1 = 0$	$\nabla \rho_e = 0$	$\phi = 0$

For the c and d boundaries, it was necessary to assign special conditions. The c boundary was defined as an opening, in a way that both the internal and external fluids could flow freely through it. This opening condition demands specific boundary conditions. Among them are: the pressure, defined by the *totalPressure* command, which consists in a fixed value condition calculated from a p_0 pressure (specified previously) and a local velocity; the velocity, defined by the *pressureInletOutletVelocity* command, which applies a zero gradient for all components except in locations where there is inflow, where, in this case, a fixed value condition was applied to the tangential component; and the volume fraction, defined by the *inletOutlet* command, which is given by a zero gradient when there is outflow, and for a fixed value when there is inflow.

The d boundary was defined with a symmetry condition. That condition implies a zero fixed value to the component of the gradient normal to the boundary, and the parallel ones are given by the projection of the components internal to the domain (Jasak, 1996).

3. RESULTS AND DISCUSSIONS

In this section the results for Newtonian and viscoelastic drops are be presented. At the first subsection, the electric field visualization and the deformation of a Newtonian drop due to the increase of the electric potential are shown. Next, the effect of different relaxation times on the viscoelastic drop deformation was compared to the Newtonian one.

3.1 Newtonian droplet

In order to evaluate the numerical solutions, analytical expressions were used. Taylor (1966) affirms that the electric potentials inside the drop ϕ_1 and outside ϕ_2 vary, in polar coordinates, according to the equations:

$$\phi_1 = E_\infty \frac{3r\cos\theta}{2 + R} \tag{19}$$

N. C. Lima, M. A. d'Ávila
Electric Effects on Conducting Newtonian and Viscoelastic Droplets

$$\emptyset_2 = E_\infty \cos\theta \left(r + \frac{1-R}{2+R}\frac{R_d^3}{r^2} \right) \tag{20}$$

where r represents the variation of the distance from the center of the sphere to the upper plate, R represent the ratio between the conductivities, R_d the sphere radius and E_∞ the external electric field.

The electric field $\boldsymbol{E}$ can be calculated using Eq. (8). Thus, the expressions of $\boldsymbol{E}$ for the normal and tangential components for the inner and outer fluids are:

$$\boldsymbol{E_{1n}} = \frac{\partial\emptyset_1}{\partial r} = \frac{3E_\infty \cos\theta}{2+R} \tag{21}$$

$$\boldsymbol{E_{1t}} = \frac{\partial\emptyset_1}{\partial\theta} = -E_\infty \sin\theta \frac{3r}{2+R} \tag{22}$$

$$\boldsymbol{E_{2n}} = \frac{\partial\emptyset_2}{\partial r} = E_\infty \cos\theta \left[1 + \frac{2(R-1)}{2+R}\frac{R_d^3}{r^3} \right] \tag{23}$$

$$\boldsymbol{E_{2t}} = \frac{\partial\emptyset_2}{\partial\theta} = -E_\infty \sin\theta \left[r + \frac{1-R}{2+R}\frac{R_d^3}{r^2} \right] \tag{24}$$

where the n and t indexes represents the normal and tangential components, respectively.

By the Eq. (21) to (24) we can observe that the normal electric field inside the sphere remains constant for a constant value of R. However, the normal electric field outside the sphere varies with the distance r. So, as $r \to \infty$ we have $E_{2n} \to E_\infty$. Those are consistent forecasts, because far from the droplet the electric field isn't affected.

The tangential components, when evaluated at the surface of the sphere, that is to say, when $r = R_d$, both values of the electric field inside and outside the droplet are the same. That's also consistent, once on any surface, the tangential components of the electric field inside and outside that surface must be the same (Griffiths, 1999).

Figure 4 shows the simulation result for the electric field using the values of $R = 2.5$, $Q = 2$ and the electric potential $\phi = 10$ kV.
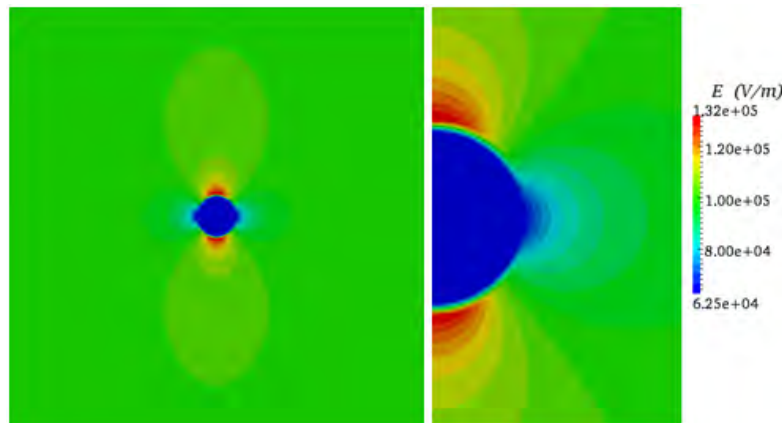

Figure 4. Electric field E around a conducting drop.

Inside the drop the electric field remains constant and outside it varies with the distance. Those results were consistent with analytical ones. As expected, far from the drop, the electric field tends to the external electric field value. Near the drop are the largest values of E, because that's where the charge accumulates. Since the direction of the external electric field E_∞ goes from top to bottom, the accumulation occurs at the upper and lower section of the drop, leaving almost no charges on the sides. In this case, the electric force will also be higher on the upper and lower parts of the drop, and, eventually, will put it in motion, deforming the drop.

In order to analyze the influence of the applied voltage on the deformation of the drop, the parameters R and Q were maintained constant and the value of Ca_E was varied. By varying the voltage, the external electric field E_∞ is also varied, and, as a consequence, the capillary number is altered. Thus, it is possible to compare the analytical solution for the deformation D (Eq. (18)) with that obtained by the simulation (Eq. (17)).

Figure 5 shows the comparison between analytical and simulation results for the droplet deformation. The values of R, Q and β were maintained equal to 2.5, 2.0 and 1.0, respectively. The value of Ca_E was varied from 0.1 to 2.5.
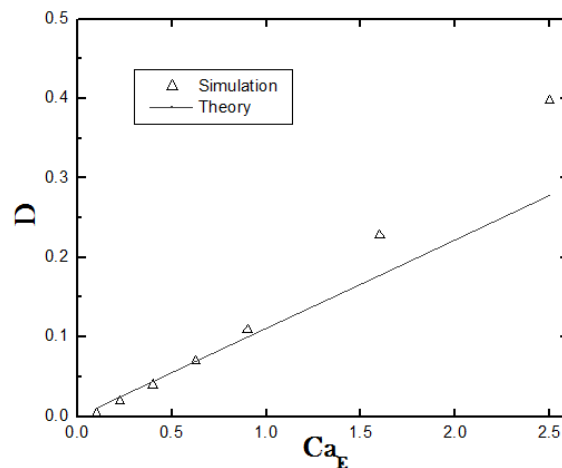
Figure 5. Diagram of the droplet deformation D versus the capillary number Ca_E.

For low values of Ca_E the simulation agrees very well with analytical results. For large deformations the simulation shows some discrepancy. However, as observed by Ha and Yang (2000), and posted by Taylor (1966), the Eq. (18) is only valid for small deformations. In fact, Hua, *et al.* (2008) also obtained discrepant results for Ca_E valued, even though they used a factor of $9/8$ instead of $9/16$ in Eq. (18).

The increase of the electric capillary number implies on a raise of the electric tensions with respect to the surface tension. Thus, the higher the value of Ca_E, the higher the deformation will be, until they reach a balance. Figure 6 displays the deformation of the drop for three different voltages:
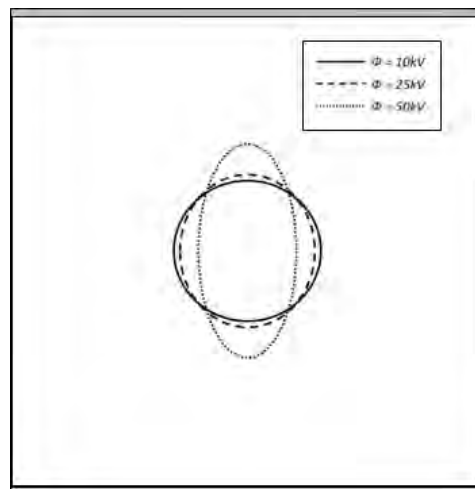

Figure 6. Deformation of the droplet varying the voltage.

As the voltage raises the droplet is changed into a prolate shape, and $D > 0$ as shown in Fig. 5. In fact, with high values of the electric potential, the electric force becomes higher too, reducing the effect of the surface tension and, consequently, increasing the deformation.

3.2 Viscoelastic droplet

The elastic parameters were evaluated with respect to a non-Newtonian droplet deformation immersed in a Newtonian fluid. The interest in analyzing the deformation is to observe the influence of the elasticity in the droplet deformation. Ha and Yang (1999) reported an experimental research about the deformation of a non-Newtonian droplet, and it was observed that the viscoelastic fluid tends to deform less than a Newtonian one. Indeed, the elastic properties retain the deformation preventing the droplet expansion.

Two comparisons were made in order to evaluate the viscoelastic effects. Initially, the deformation of a viscoelastic drop was compared to the Newtonian one. To do so, the relaxation time λ was maintained fixed as the electric capillary

number was varied. Four different values of λ were used, that implies four different non-Newtonian fluids. The relaxation times varied from $10^0 \leq \lambda \leq 10^{-3}$, and the results were compared to the results of Fig. 5.

For a second analysis, the capillary number was maintained constant and the relaxation time was varied, in order to evaluate the influence of elasticity on the drop deformation.

Since we are looking for the influence of viscoelastic properties, the electric parameters were maintained constant. Among them, are the perrmittivity ratio $Q = 2$ and the conductivity ratio, $R = 2.5$. The fluids (Newtonian being the outer fluid and non-Newtonian being the inner one) have the same density, and the ratio of viscosities was equal to one $\beta = \eta_P / \mu = 1$. It is important to notice that the viscosities ratio is the viscosity at zero share rate for the viscoelastic fluid over the dynamic viscosity of the Newtonian fluid.

Figure 7 presents the comparison between the deformation of a Newtonian fluid with four different viscoelastic fluids:
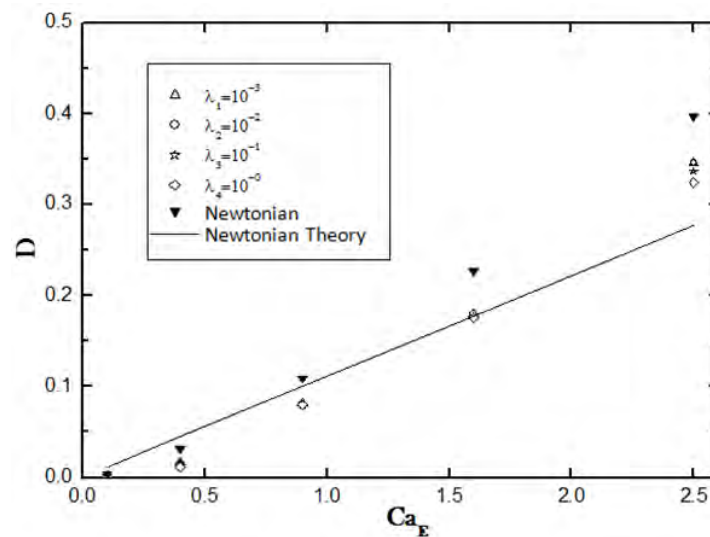

Figure 7. Comparison of a viscoelastic drop deformation varying the capillary number for four different values of λ, with the results obtained by a Newtonian drop (Fig. 5).

The results show that a viscoelastic drop deforms less than a Newtonian one. As pointed by Ha and Yang (2000), the elastic properties of the fluid tends to compress it, raising its stability with respect to the deformation. Their experimental data shows the same behavior for non-Newtonian fluids.

Another observation that can be made about Fig. 7 is that an increase in the relaxation time implies in a decrease on the deformation D of the droplet. Indeed, an increase on λ, implies in an increase on the *Deborah number De*, given by Eq. (25). The last one, is directly associated with the elastic properties of the fluid, once, the higher the *Deborah number*, the higher the elasticity of the fluid, and the lower the value of De, more the fluid tends to behave itself as a purely viscous fluid.

$$De = \frac{\lambda}{t_c} \tag{25}$$

In Eq. (25) λ is the relaxation time and t_c is the characteristic experiment time.

Clearly the influence of the relaxation time is more accentuated for large deformations in Fig. 7. The explanation is that for low values of λ, such as λ_1 and λ_2, the drop behave more like a Newtonian fluid and, as a consequence, its deformation is closer to those for Newtonian ones. Another fact is that, as pointed by Ha and Yang (2000), even viscoelastic drop (or purely elastic) deformation match with the drop deformation theory of Newtonian fluids for small deformations.

In other words, independently if the fluid is viscoelastic or not, when considering small deformations it tends always on the same values of the D. The Diagram below, Fig. 8, shows exactly the last statement.
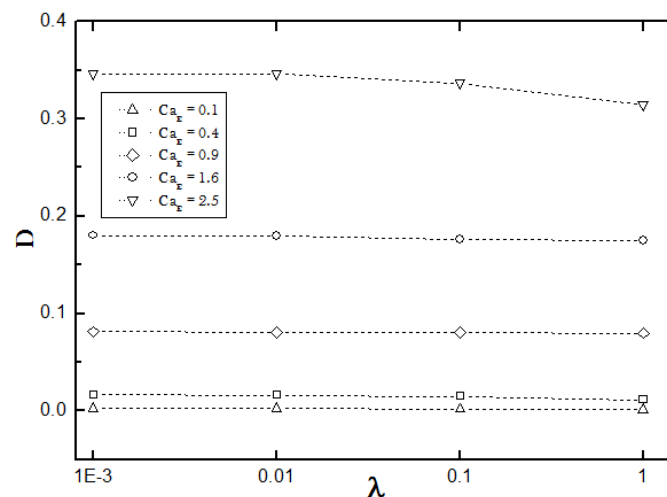
Figure 8. Comparison of the droplet deformation varying λ for different values of Ca_E.

As we can see, for small values of D the relaxation time almost no influence. However, for large deformations as the fluid becomes more elastic (large values of λ) the deformation has a greater variation. Nevertheless, it is possible to state that the electric field still is the parameter that has most influence on the drop deformation.

4. CONCLUSION

This work presented the implementation of the leaky dielectric model in the free open source package OpenFOAM, in order to simulate electrohydrodynamic flows of Newtonian and non-Newtonian fluids. The solver *viscoelasticInterFoam* developed by Favero, *et al.* (2010b) was changed with the inclusion of the equations related to electrohydrodynamic problems. The classic problem about the deformation of a droplet was simulated, so that the new solver could be validated. The results showed good agreement with the analytical model and also with observations made by other authors. The electric field around the drop behaved as expected with the largest values near the points where the charge density was located and tending to the external electric field far from the drop. The deformation of the Newtonian droplet was consistent with analytical results for small deformations. For large deformations some discrepancy was observed, however, the same results can be seen in literature. In order to describe the viscoelastic behavior, the Giesekus model was used. Differently from Newtonian fluids, there are few works in literature that investigates the influence of electric effects on viscoelastic drops. Notwithstanding, the results obtained by the simulations agreed with experimental observations. The elasticity of the fluid had an influence on the drop deformation by reducing it. For large deformations it was observed that the increase of the relaxation time reduced the deformation, but for small values of D, the relaxation time variation had almost no influence on it. Thus, the solver functioned according to expectations showing capability for dealing either with Newtonian or viscoelastic fluids.

5. ACKNOWLEDGEMENTS

6. REFERENCES

BIRD, R. B.; ARMSTRONG, R. C.; HASSAGER, O., 1987. *Dynamics of Polymeric Liquids.* Jhon Wiley & Sons, New York, 2nd . edition.

FAVERO, J. L.; SECCHI, A. R.; CARDOZO, N. S. M.; JASAK, H., 2010a. "Viscoelastic flow analysis using the software OpenFOAM and differential constitutive equations". *Journal of Non-Newtonian Fluid Mechanics*, Vol. 165, p. 1625-1636.

FAVERO, J. L.; SECCHI, A. R.; CARDOZO, N. S. M.; JASAK, H. , 2010b. "Viscoelastic fluid analysis in internal and in free surface flows using the software OpenFOAM". *Computers and Chemical Engineering*, Vol. 34, p. 1984-1993.

FAVERO, J. L.; 2009. *Simulação de escoamentos viscoelásticos: Desenvolvimento de uma Metodologia de Análise utilizando o Software OpenFOAM e Equações Constitutivas Diferenciais*. Mestres Thesis, UFRGS, Porto Alegre, RS.

FENG, J. J., 2002. "The stretching of an electrified non-Newtonian jet: A model for electrospinning". *Physics of Fluids*, Vol. 14, No. 11, p. 3912-3926.

FENG, J. Q.; SCOTT, T. C. , 1996. "A computational analysis of electrohydrodynamics of a leaky dielectric drop in an electric field". *J. Fluid Mech.*, Vol. 311, p. 289-326.

GIESEKUS, H. , 1982. "A simple constitutive equation for polymer fluids based on the concept of deformation-dependent tensorial mobility", *Journal of Non-Newtonian Fluid Mechanics*, Vol. 11, No. 1-2, p. 69-109.

GRIFFITHS, D. J., 1999. *Introduction to Electrohydrodynamics.* Prentice-Hall Inc., Upper Saddle River, New Jersey 3rd edition.

HA, J.-W.; YANG, S.-M. , 1999. "Deformation and Breakup of a Second-Order Fluid in an Electric Field". *Korean J. Chem. Eng.*, Vol. 16, p. 585-594.

HA, J.-W.; YANG, S.-M., 2000. "Deformation and breakup of Newtonian and non-Newtonian conducting drops in an electric field", *J. Fluid Mech.*, Vol. 405, p. 131-156.

HA, J.-W.; YANG, S.-M., 1995. "Effects of surfactant on the deformation and stability of a drop in viscous fluid in an electric field". *J. Colloid Interface Sci.*, Vol. 175, p. 369-385.

HERRERA, J. M. L.; POPINET, S.; HERRADA, M. A., 2011. "A charge-conservative approach for simulating electrohydrodynamic two-phase flows using volume-of-fluid". *Journal of Computational Physics.* Vol. 230, p. 1939-1955.

HIRT, C. W.; NICHOLS, B. D., 1981. "Volume of Fluid (VOF) Method for the Dynamics of Free Boundaries", *Journal of Computational Physics*, Vol. 39, p. 201-225.

HUA, J.; LIM, L. K.; WANG, C., 2008. "Numerical simulation of deformation/motion of a drop suspended in viscous liquids under influence of steady electric fields", *Physics of Fluids*, Vol. 20, p. 113302.

JASAK, H., 1996. *Error Analysis and Estimation for the Finite Volume Method with Applications to Fluid Flows.* Ph.D thesis, Imperial College of Science, University of London, London.

POPPEL, B. P. V., 2010. *Numerical Methods for Simulating Multiphase Electrohydrodynamic Flows with Application to Liquid Fuel Injection.* Ph.D thesis, University of Colorado, Department of Mechanical Engineering, Colorado.

SAVILLE, D. A., 1997. "Electrohydrodynamics: The Taylor-Melcher Leaky Dieletric Model". *Annu. Rev. Fluid Mech.*, Vol. 29, p. 27-64.

SHERWOOD, J. D., 1988. "Breakup of fluid droplets in electric and magnetic fields", *Journal of Fluid Mech.*, Vol. 188, p. 133-146.

TAYLOR, G., 1964. "Disintegration of Water Drops in an Electric Field". *Proceedings of the Royal Society of London. Series A, Mathematical and Physical Sciences*, Vol. 280, No. 1382. p. 383-397.

TAYLOR, G.; McEWAN, A. D.; JONG, L. N. J., 1966. "Studies in electrohydrodynamics I. The circulation produced in a drop by an electric field", *Proceedings of the Royal Society of London. Series A, Mathematical and Physical Sciences*, Vol. 291, No. 1425, p. 159-166.

THOMPSON, C. J.; CHASE, G. G.; YARIN, A. L.; RENEKER, D. H., 2007. "Effects of parameters on nanofiber diameter determined from electrospinning model", *Polymer*, Vol. 48, p. 6913-6922.

TOMAR, G.; GERLACH, D.; BISWAS, G.; ALLEBORN, N.; SHARMA, A.; DURST, F.; WELCH, S. W. J.; DELGADO, A., 2007. "Two-phase electohydrodynamic simulations using a volume-of-fluid approach", *Journal of Computational Physics*, Vol. 227, p. 1267-1285.

7. RESPONSIBILITY NOTICE

The authors are the only responsible for the printed material included in this paper.